

# R recoilless Resonant Absorption of Monochromatic Neutrino Beam for Measuring $m_{31}^2$ and $\sin^2 2_{13}$

Hisakazu Minakata<sup>1,2</sup> and Shoichi Uchinaru<sup>1,y</sup>

<sup>1</sup>Department of Physics, Tokyo Metropolitan University

1-1 Minamiohisa, Hachioji, Tokyo 192-0397, Japan

<sup>2</sup>Abdus Salam International Center for Theoretical Physics,  
Strada Costiera 11, 34014 Trieste, Italy

(Dated: February 6, 2006)

## Abstract

We discuss, in the context of precision measurement of  $m_{31}^2$  and  $\sin^2 2_{13}$ , physics capabilities enabled by the recoilless resonant absorption of monochromatic antineutrino beam enhanced by the Mossbauer effect recently proposed by Raghavan. Under the assumption of small relative systematic error of a few tens of percent level between measurement at different detector locations, we give analytical and numerical estimates of the sensitivities to  $m_{31}^2$  and  $\sin^2 2_{13}$ . The accuracies of determination of them are enormous; The fractional uncertainty in  $m_{31}^2$  achievable by 10 point measurement is 0.6% (2.4%) for  $\sin^2 2_{13} = 0.05$ , and the uncertainty of  $\sin^2 2_{13}$  is 0.002 (0.008) both at 1 CL with the optimistic (pessimistic) assumption of systematic error of 0.2% (1%). The former opens a new possibility of determining the neutrino mass hierarchy by comparing the measured value of  $m_{31}^2$  with the one by accelerator experiments, while the latter will help resolving the  $_{23}$  octant degeneracy.

PACS numbers: 14.60.Pq, 25.30.Pt, 76.80.+y

---

<sup>x</sup>Electronic address: Email: minakata@phys.metro-u.ac.jp

<sup>y</sup>Electronic address: Email: uchinaru@phys.metro-u.ac.jp

## I. INTRODUCTION

Recently, an intriguing possibility was suggested by Raghavan [1, 2] that the resonant absorption reaction [3]



with simultaneous capture of an atomic orbital electron can be dramatically enhanced. The key idea is to use monochromatic  $e^-$  beam with the energy 18.6 keV from the inverse reaction  ${}^3\text{H} \rightarrow e^- + {}^3\text{He} + \text{orbitale}$ , by which the resonance condition is automatically satisfied. He then suggested an experiment to measure  $m_{13}$  by utilizing the ultra low-energy monochromatic  $e^-$  beam. Though similar to the reactor  $m_{13}$  experiments [4, 5, 6], the typical baseline length is of order 10 m due to much lower energy of the beam by a factor of 150, making it doable in the laboratories. The mechanism, in principle, would work with more generic setting in which  ${}^3\text{H}$  and  ${}^3\text{He}$  in (1) are replaced by nuclei  $A$  ( $Z$ ) and  $A$  ( $Z-1$ ).

The author of [1, 2] then went on to even more aggressive proposal of enhancement by a factor of  $10^4$  by embedding both  ${}^3\text{H}$  and  ${}^3\text{He}$  into solids by which the broadening of the beam due to nuclear recoil is severely suppressed by a mechanism similar to the Mossbauer effect [7]. Then, the event rate of the  $m_{13}$  experiment is enhanced by the same factor, allowing extremely high counting rate. Thanks to the ultimate energy resolution of  $E = E' / 2 = 10^{17}$  enabled by the recoilless mechanism, he was able to propose a tabletop experiment to measure gravitational red shift of neutrinos, a neutrino analogue of the Pound-Rebka experiment for photons [8].

In this paper, we examine the possible physics potential of the  $m_{13}$  experiment proposed in [1, 2]. The characteristic feature of the experiment, which clearly marks the difference from the reactor  $m_{13}$  measurement, is the use of monochromatic beam apart from the shorter baseline by a factor of 150. Then, the most interesting question is how accurately  $m_{31}^2$  can be determined. Note that even without recoilless setting, the beam energy width is of the order of  $E = E' / 10^5$ , and it can be ignored for all practical purposes. It is also interesting to explore the accuracy of  $m_{13}$  measurement. In addition to possible extremely high statistics, the baseline as short as 10 m should allow us to utilize the movable detector technique, the one which once proposed in a reactor  $m_{13}$  experiment [9] but the one that did not survive in the (semi-)final proposal. The method will greatly help to reduce the experimental systematic uncertainties of the measurement.

We will show in our analysis that the accuracies one can achieve for  $m_{31}^2$  and  $m_{13}$  determination by the recoilless resonant absorption are enormous. At  $\sin^2 2_{13} = 0.05$ , for example, the fractional uncertainty in  $m_{31}^2$  determination is 0.6% (2.4%) and the uncertainty of  $\sin^2 2_{13}$  is 0.002 (0.008) both at 1 CL under an optimistic (pessimistic) assumption of systematic error of 0.2% (1%).

What is the scientific merit of such precision measurement of  $m_{31}^2$  and  $m_{13}$ ? With a 1% level precision of  $m_{31}^2$ , the method for determining neutrino mass hierarchy by comparing between the two effective  $m^2$  measured in reactor and accelerator (or atmospheric) disappearance measurement [10, 11] would work, opening another door for determining the neutrino mass hierarchy. It is also proposed [5] that the  $m_{23}$  octant degeneracy can be resolved by combining reactor measurement of  $m_{13}$  with accelerator appearance (disappearance) measurement of  $s_{23}^2$  ( $\sin^2 2_{13}$ ). (See [12, 13] for earlier qualitative suggestions.) The results of the recent quantitative analysis [14], however, indicate that the resolving power of the method is limited at small  $m_{13}$  primarily because of the uncertainties in reactor measurement of  $m_{13}$ . Therefore, the highly accurate measurement of  $m_{31}^2$  and  $m_{13}$  which is enabled

by using resonant absorption reaction should help resolving the mass hierarchy and the  $m_{23}$  degeneracies.

In Sec. II, we discuss "conceptual design" of the possible experiments. In Sec. III, we define the statistical method for our analysis. In Sec. IV, we present numerical analysis of the sensitivities of  $m_{13}$  and  $m_{31}^2$  measurement. In Sec. V, we complement the numerical estimate in Sec. IV by giving analytic estimate of the sensitivities. In Sec. VI, we give some remarks on implications of our results. In Appendix A, we give a general formula for the inverse of the error matrix.

## II. WHICH KIND OF $m_{13}$ EXPERIMENT?

We give preliminary discussions on which kind of setting is likely to be the best one for experiment to measure  $m_{31}^2$  and  $m_{13}$  with use of ultra low-energy monochromatic  $e^-$  beam. In this section, we rely on the one-mass scale dominant [15] (or the two-flavor) approximation of the neutrino oscillation probability  $P(e^- \rightarrow e^-)$ , though we use the full three-flavor expression in our quantitative analysis performed in Sec. IV. It reads

$$P(e^- \rightarrow e^-) = 1 - \sin^2 2 \cdot m_{13}^2 \cdot \frac{m_{31}^2 L}{4E}; \quad (2)$$

where the neutrino mass squared difference is defined as  $m_{ji}^2 = m_j^2 - m_i^2$  with neutrino masses  $m_i$  ( $i = 1-3$ )<sup>1</sup> and  $L$  is a distance from a source to a detector. With  $E = 18.6$  keV, the first oscillation maximum (minimum in  $P(e^- \rightarrow e^-)$ ) is reached at the baseline distance

$$L_{OM} = 9.2 \cdot \frac{m_{31}^2}{2.5 \cdot 10^3 \text{ eV}^2} \quad \text{m}; \quad (3)$$

While the current value of  $m_{31}^2$  which comes from the atmospheric [16] and the accelerator [17] measurement has large uncertainties, it should be possible to narrow down the value thanks to the ongoing and the forthcoming disappearance measurement by MINOS [18] and T2K [19] experiments. Furthermore, the experiment considered in this paper is powerful enough to determine both quantities accurately at the same time, if detector locations are appropriately chosen.

The whole discussion of the  $m_{13}$  experiment must be preceded by the test measurement at 10 cm or so to verify the principle, namely to demonstrate that the mechanism of resonant enhancement proposed in [1, 2] is indeed at work. At the same time, the flux times cross section must be measured to check the consistency of the Monte Carlo estimate. Then, one can go on to the measurement of  $m_{13}$  and  $m_{31}^2$ , and possibly other quantities. Because of the expected high statistics of the experiment it is natural to think about using spectrum informations. In the case of monochromatic beam it amounts to consider measurement at several different detector locations.

---

<sup>1</sup> When we speak about discriminating the neutrino mass hierarchy by comparing the two "large"  $m^2$  measured in  $e^-$  disappearance and  $\bar{e}$  disappearance channels, one has to be careful about the definition of  $m^2$  which enter into the survival probabilities [10]. While keeping this point in mind, we do not try to elaborate the expressions of  $m^2$  by just writing it in  $e^-$  disappearance channel as  $m_{31}^2$  in this paper.

Let us estimate the event rate. Although the precise rate is hard to estimate, the numbers displayed below will give the readers a feeling on what would be the time scale for the experiment. The flux from  ${}^3\text{H}$  source with strength  $\text{SM Ci}$  due to bound state beta decay is given by

$$f_e = 1.4 \times 10^7 \frac{S}{\text{1M Ci}} \frac{L}{10 \text{ m}}^2 \text{ cm}^2 \text{ s}^{-1} \quad (4)$$

where the ratio of bound state beta decay to free space decay is taken to be  $4.7 \times 10^3$  based on [20]. The rate of the resonant absorption reaction can be computed by using cross section  $\sigma_{\text{res}}$  and number of target atoms  $N_T$  as  $R = N_T f_e \sigma_{\text{res}}$ . Without the Mossbauer enhancement the cross section is estimated to be  $\sigma_{\text{res}} \approx 10^{-42} \text{ cm}^2$  [1]. Then, the rate with target mass  $M_T$  is given by

$$R = 2.4 \times 10^4 \frac{\text{SM}_T}{\text{1M Ci}} \frac{L}{10 \text{ m}}^2 \text{ day}^{-1} \quad (5)$$

An improved estimate in [2] entailed a factor of  $\approx 10^{11}$  enhancement of the cross section by the Mossbauer effect after the source and the target are embedded into solids. Assuming the enhancement factor,  $\sigma_{\text{res}} \approx 10^{-31} \text{ cm}^2$  and the rate becomes

$$R_{\text{enhanced}} = 2.4 \times 10^4 \frac{\text{SM}_T}{\text{1M Ci}} \frac{L}{10 \text{ m}}^2 \text{ day}^{-1} \quad (6)$$

Therefore, one obtains about  $2.4 \times 10^6$  events per day for 1 M Ci source and 100 g  ${}^3\text{He}$  target at a baseline distance  $L = 10 \text{ m}$ . If the enhancement factor is not reached the running time for collecting the same number of events becomes longer accordingly.

Thus, once the  ${}^3\text{He}$  (and much easier  ${}^3\text{H}$ ) implantation into solid is achieved, the event rate is sufficient. The real issue for high sensitivity in  $m_{31}^2$  and  $\sin^2 2_{13}$  measurement is whether the produced  ${}^3\text{H}$  can be counted directly without waiting for decaying into  ${}^3\text{He}$  by emitting electron. It is because the long lifetime of 12.33 year [21] of  ${}^3\text{H}$  makes it impossible to identify which period the decayed  ${}^3\text{H}$  was produced, resulting in the errors of the event rate in each detector location. Possibilities of real-time counting and direct counting by extracting  ${}^3\text{H}$  atoms are mentioned in [2]. In this paper, we assume that at least one of such methods works, and it offers opportunity of direct counting of events. Note that the detection efficiency need not be high because of huge number of events. What is important is the time-stable counting rate which allows relative systematic errors between measurement at different detector locations small enough.

### III. STATISTICAL METHOD FOR ANALYSIS

In this section, we define the statistical procedure for our analysis to estimate the sensitivities of  $m_{31}^2$  and  $\sin^2 2_{13}$  to be carried out in the following sections. We aim at illustrating general properties of the  $\chi^2$  under the assumption of the small uncorrelated systematic errors compared to the correlated ones.

## A . Definition of $\chi^2$ and characteristic properties of errors

We consider measurement at  $n$  different distances  $L = L_i$  ( $i = 1, 2, \dots, n$ ) from the source. Then, the appropriate form of  $\chi^2$  which is suited for analytic study [22] and is simply denoted as  $\chi^2$  hereafter, is as follows:

$$\chi^2 = \sum_{i=1}^n \frac{N_i^{\text{obs}} - (1 + \epsilon_i) N_i^{\text{exp}}}{N_i^{\text{exp}} + (\epsilon_{\text{sys};i} N_i^{\text{exp}})^2} + \frac{\epsilon^2}{\epsilon_c^2} \quad (7)$$

where  $N_i^{\text{obs}}$  is the number of events computed with the values of parameters given by nature, and  $N_i^{\text{exp}}$  is the one computed with certain trial set of parameters.  $\epsilon_c$  is the systematic error common to measurement at  $n$  different distances, the correlated error, whereas  $\epsilon_{\text{sys};i}$  indicate errors that cannot be attributed to  $\epsilon_c$ , the uncorrelated errors. The example of the former and the latter errors are as follows:

$\epsilon_c$  (correlated error): Uncertainties in number of target  ${}^3\text{H}$  atoms, errors in counting the number of produced tritium nuclei, errors in calculating resonant absorption cross section, errors in estimating the efficiency of counting tritium nuclei

$\epsilon_{\text{sys};i}$  (uncorrelated error) : Possible time dependence of number of decaying tritium nuclei and detection efficiency of events

Since we consider moving detector setting the list of the thinkable uncorrelated systematic errors is quite limited. If the near detector with the identical structure with a movable far detector exists the error can, in principle, be vanishingly small. One may think of the errors of the order of 0.1% - 0.3%. It is because the flux times cross section can be monitored in real time by a near detector. In fact, the similar values for uncorrelated systematic error are adopted in sensitivity estimate of some of the reactor  ${}_{13}\text{C}$  experiments such as the Braiwood, the Daya Bay, and the Angra projects [23, 24, 25]. In near future experiments, somewhat larger values are taken, 0.6% in Double-Chooz project [26] and 0.35% in KASKA [27].

On the other hand, it may not be so easy to control the correlated systematic error  $\epsilon_c$ . The number of  ${}^3\text{H}$  nuclei may be measured when they are implanted into solid. The number of target nuclei times the resonant absorption cross section may be measured in a research and development stage with a near detector. Therefore, we suspect that the largest error may come from uncertainty in counting rate of the produced  ${}^3\text{H}$  nuclei. Of course, reliable estimate of systematic errors  $\epsilon_c$  and  $\epsilon_{\text{sys}}$  requires specification of the site to estimate the background caused by  ${}^3\text{H}$  reaction etc. But, it can be experimentally measured by the source on and off procedure, as pointed out in [1]. Lacking definitive numbers for  $\epsilon_c$  at the moment, we use a conservative value  $\epsilon_c = 10\%$  throughout our analysis.

If the direct counting of  ${}^3\text{H}$  atoms does not work, we may have to expect much larger systematic errors, because one has to extract event rate at each detector location only by fitting the decay curve. Probably, the better strategy without the direct counting would be to place multiple identical detectors (or of the same structure) at appropriate baseline distances. Even in this case, it is quite possible that the uncorrelated systematic error  $\epsilon_{\text{sys}}$  can be controlled to 1% level, as expected in a variety of reactor  ${}_{13}\text{C}$  experiments [6]. At the moment, we do not know how large are  $\epsilon_c$  and  $\epsilon_{\text{sys}}$  in this case. Furthermore, determination of baseline dependent event rates would be more and more difficult for larger number of detector locations.

## B. Approximate form of $\chi^2$ with hierarchy in errors

By eliminating  $\chi^2$  through minimization the  $\chi^2$  can be written as

$$\chi^2 = \mathbf{x}^T V^{-1} \mathbf{x} \quad (8)$$

where  $\mathbf{x}$  is defined as

$$\mathbf{x}^T = \frac{N_1^{\text{obs}} - N_1^{\text{exp}}}{N_1^{\text{exp}}}; \frac{N_2^{\text{obs}} - N_2^{\text{exp}}}{N_2^{\text{exp}}}; \frac{N_n^{\text{obs}} - N_n^{\text{exp}}}{N_n^{\text{exp}}} \dots \quad (9)$$

Using the general formula given in Appendix A,  $V^{-1}$  is given by

$$(V^{-1})_{ij} = \frac{\frac{ij}{2}}{\frac{1}{ui}} - \frac{1}{\frac{2}{ui} \frac{2}{uj} \frac{1}{1 + \sum_{k=1}^n \frac{1}{\frac{2}{uk}}}} \frac{2}{c} \quad (10)$$

where  $\frac{2}{ui} = \frac{2}{\text{usys};i} + \frac{1}{N_i^{\text{exp}}}$ . By construction, the  $\chi^2$  depends upon  $\text{usys};i$  and  $N_i^{\text{exp}}$  only through this combination. Therefore, the particular case that will be taken in the next section, in fact, includes many cases with different event number but with the same  $c$ .

Under the approximation  $\frac{2}{ui} \approx \frac{2}{c}$ ,  $V^{-1}$  simplifies;

$$(V^{-1})_{ij} = \frac{\frac{ij}{2}}{\frac{1}{ui}} - \frac{1}{\frac{2}{ui} \frac{2}{uj} \frac{1}{1 + \sum_{k=1}^n \frac{1}{\frac{2}{uk}}}} \quad (11)$$

The remarkable feature of (11) is the "scaling behavior" in which  $\chi^2$  is independent of the correlated error  $c$ , and the sensitivity to  $\sin^2 \theta_{13}$  and  $\sin^2 \theta_{31}$  can be made higher as the uncorrelated systematic errors as well as the statistical error become smaller. It may be counterintuitive because the leading term of the error matrix  $V$  is of order  $\frac{2}{c}$ . (See Appendix A.) It is due to the singular nature of the leading order matrix, as noted in [28].

## IV. ESTIMATION OF SENSITIVITIES OF $\sin^2 \theta_{31}$ AND $\sin^2 \theta_{13}$

We now examine the sensitivities of  $\sin^2 \theta_{31}$  and  $\sin^2 \theta_{13}$  achievable by recoilless resonant absorption of monochromatic  $e^-$  enhanced by the Mossbauer effect. The numerical estimate of the sensitivities in this section will be followed by the one by the analytic method in Sec. V.

The setting of movable detector and the expected high statistics of the experiment make it possible to consider the situation that an equal number of events are taken in each detector location. Of course, the far a detector from the source, the longer an exposure will take. In the following analysis, the number of events are assumed to be  $10^6$  in each detector location. Given the rate in (6), and assuming that the direct counting works, it is obtainable in 10 days for 100 g  $^3\text{He}$  target even if the detector is located at the second oscillation maximum,  $L = 3L_{\text{OM}}$ . On the other hand, the number of events  $10^6$  is sufficient for our purpose because it is unlikely that the uncorrelated systematic errors can be made much smaller than 0.1%.

We take a "common-sense approach" to determine the locations of the detectors and postpone the discussion of the optimization problem. We examine the following four types of run, Run I, IIA, IIB, and III, for the measurement.

Run I: Measurement at 5 detector positions,  $L = \frac{1}{5}L_{OM}, \frac{3}{5}L_{OM}, L_{OM}, \frac{7}{5}L_{OM},$  and  $\frac{9}{5}L_{OM}$  are considered so that  $m_{31}^2 L = 4E = 10; 3 = 10; 2; 7 = 10; 9 = 10$  are covered.

Run IIA : An extreme setting for precision determination of  $m_{31}^2$  by measurement at 10 detector positions:  $L = L_i$  ( $i = 1, \dots, 10$ ) where  $L_{i+1} = L_i + \frac{1}{5}L_{OM}$  and  $L_1 = \frac{1}{5}L_{OM}$  so that the range  $= 0$  to  $\pi$  is covered.

Run IIB : An extreme setting for precision determination of  $m_{31}^2$  by measurement at 10 detector positions:  $L = L_i$  ( $i = 1, \dots, 10$ ) where  $L_{i+1} = L_i + \frac{2}{5}L_{OM}$  and  $L_1 = \frac{1}{5}L_{OM}$  so that the entire period,  $= 0$  to  $2\pi$ , is covered.

Run III: A somewhat extreme setting of 20 detector positions  $L = L_i$  ( $i = 1, \dots, 20$ ) where  $L_{i+1} = L_i + \frac{1}{5}L_{OM}$  and  $L_1 = \frac{1}{5}L_{OM}$  ( $= 0 \dots 2\pi$ ). It is to check the scaling behavior of the sensitivity with respect to errors.

In the following two subsections we examine the cases of the optimistic ( $u_{sys} = 0.2\%$ ) and the pessimistic ( $u_{sys} = 1\%$ ) systematic errors. We stress here that the analyses we will present there contain much more general cases. For example, because of the scaling behavior discussed in the previous section, the case with  $N = 10^6$  and  $u_{sys} = 0.2\%$  is equivalent to  $N = 2 \times 10^6$  and  $u_{sys} = 0.0\%$ . Similarly, the case with  $N = 10^6$  and  $u_{sys} = 1\%$  is equivalent to  $N = 1.33 \times 10^6$  and  $u_{sys} = 0.5\%$ .

### A. Case of optimistic systematic error

We focus in this subsection on the case of optimistic systematic error, from which one may obtain some feeling on the ultimate sensitivities achievable by the present method with the four Run options described above. As we mentioned earlier, the correlated systematic error  $c$  is taken to be a conservative value of 10% throughout our analysis. The uncorrelated systematic error  $u_{sys}$ , which is assumed to be equal for all detector locations, is taken to be 0.2% in this subsection.

In Fig. 1 we show in  $\sin^2 2_{13}$  –  $m_{31}^2$  plane the expected allowed region by Run I, IIA, IIB, and III with number of events  $10^6$  in each location. Throughout the analysis, the true values of  $m_{31}^2$  is assumed to be  $m_{31}^2 = 2.5 \times 10^3 \text{ eV}^2$ . The input values of  $\sin^2 2_{13}$  is taken as 0.1 and 0.01 in the left and the right panels in Fig. 1, respectively. Throughout the numerical analyses in this paper, the other oscillation parameters are taken as:  $m_{21}^2 = 7.9 \times 10^5 \text{ eV}^2$ ,  $\sin^2 2_{12} = 0.31$ , and  $\sin^2 2_{23} = 0.5$ . In each panel, the red-solid, the green-dashed, and the blue-dotted lines are for 1 (68.27%), 2 (95.45%), and 3 (99.73%) CL for 2 DOF (degrees of freedom), respectively.

To complement Fig. 1, we give in Table I the expected sensitivities for  $m_{31}^2$  at 1 and 3 CL (the latter in parentheses) for 1 DOF for Run I-III. They are obtained by optimizing  $\sin^2 2_{13}$  in the  $t$ . For relatively large  $2_{13}$ ,  $\sin^2 2_{13} > 0.05$  the expected sensitivities for  $m_{31}^2$  are enormous. For  $\sin^2 2_{13} = 0.05$  the sensitivities are already less than 1% in Run IIA, and is about 0.6% in Run IIB both at 1 CL. The scaling behavior (to be derived in Sec. V) is roughly satisfied by the errors expected in Run IIA – III, as is indicated in Table I.

For a small value of  $2_{13}$ ,  $\sin^2 2_{13} = 0.01$  the sensitivities are much worse, as shown in Table I. They are about 6% in Run IIA, and 3% in Run IIB both at 1 CL. If Run III is carried out it can go down to 2%.

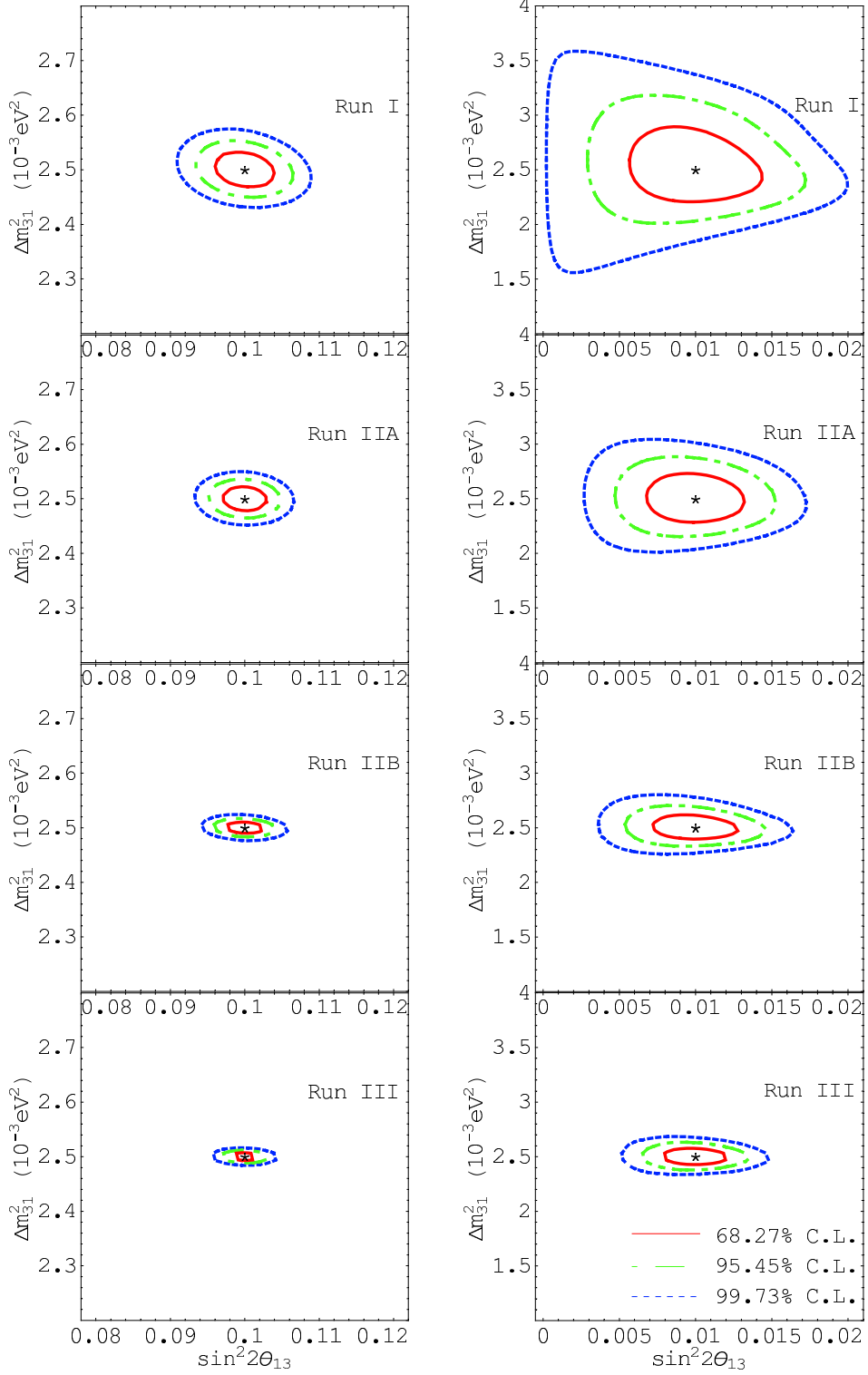


FIG. 1: The expected allowed region by Run I, IIA, IIB, and III with number of events  $10^6$  in each location are depicted. The red-solid, the green-dashed, and the blue-dotted lines are for 1 (68.27%), 2 (95.45%), and 3 (99.73%) CL for 2 DOF, respectively. The input values of the mixing parameters are marked by asterisks and they are as follows:  $m_{31}^2 = 2.5 \times 10^3 \text{ eV}^2$ ,  $\sin^2 2 \theta_{13} = 0.1$  and  $0.01$  in the left and the right panels.

TABLE I: The expected fractional uncertainty  $(m^2) = m_{31}^2(0)$  in % for the optimistic systematic error of  $u_{\text{sys}} = 0.2\%$  reachable by the Run I–III defined in the text. The uncertainties are given at 1 (68.27%) CL for 1 DOF, and the numbers in parentheses are the ones at 3 (99.73%) CL for 1 DOF. In the left, middle, and right columns, the input value of  $_{13}$  are taken as  $\sin^2 2_{13} = 0.1$ , 0.05, and 0.01, respectively.

$u_{\text{sys}} = 0.2\%$	$\sin^2 2_{13} = 0.1$	$\sin^2 2_{13} = 0.05$	$\sin^2 2_{13} = 0.01$
Run type	$(m^2) = m_{31}^2(0)$ (in %) at 1 (3) CL		
Run I (5 locations)	0.84 (2.5)	1.7 (5.0)	$9.6^{+31}_{-23}$
Run IIA (10 locations)	0.56 (1.7)	1.2 (3.5)	$6.0^{+18}_{-16}$
Run IIB (10 locations)	0.28 (0.8)	0.56 (1.6)	$2.8^{+9.6}_{-8.0}$
Run III (20 locations)	0.2 (0.56)	0.4 (1.2)	$2.0^{+6.0}_{-5.6}$

TABLE II: The expected sensitivity to the  $\sin^2 2_{13}$  for the optimistic systematic error of  $u_{\text{sys}} = 0.2\%$  reachable by the Run I–III defined in the text. The uncertainties ( $\sin^2 2_{13}$ ) are given at 1 (68.27%) CL for 1 DOF, and the numbers in parentheses are the ones at 3 (99.73%) CL for 1 DOF. In the left, middle, and right columns, the input value of  $_{13}$  are taken as  $\sin^2 2_{13} = 0.1$ , 0.05, and 0.01, respectively.

$u_{\text{sys}} = 0.2\%$	$\sin^2 2_{13} = 0.1$	$\sin^2 2_{13} = 0.05$	$\sin^2 2_{13} = 0.01$
Run type	$\sin^2 2_{13}$ at 1 (3) CL		
Run I (5 locations)	0.1 0.0026 (0.0078)	0.05 0.0027 (0.0081)	0.01 0.0028 (0.0085)
Run IIA (10 locations)	0.1 0.0019 (0.0058)	0.05 0.0020 (0.0061)	0.01 0.0021 (0.0064)
Run IIB (10 locations)	0.1 0.0017 (0.0050)	0.05 0.0018 (0.0053)	0.01 0.0018 (0.0055)
Run III (20 locations)	0.1 0.0013 (0.0038)	0.05 0.0014 (0.0041)	0.01 0.0014 (0.0042)

In Table II the expected sensitivities for  $\sin^2 2_{13}$  at 1 and 3 CL (the latter in parentheses) for 1 DOF are given. The sensitivities for  $\sin^2 2_{13}$  can be better characterized by  $(\sin^2 2_{13})$ , not its fraction to  $\sin^2 2_{13}$ , as will be understood in our analytic treatment in Sec. V. By Run I one can already achieve the accuracy of  $(\sin^2 2_{13}) \approx 0.003$ , and Run IIA or IIB reach to  $(\sin^2 2_{13}) \approx 0.002$ . The effect of measurement at multiple detector locations on improvement of the sensitivity is relatively minor in the case of sensitivities for  $\sin^2 2_{13}$ . This is in sharp contrast to the case of  $m_{31}^2$ .

To show the sensitivity limit on  $_{13}$  achievable by the present method, we present in Fig. 2 the excluded regions in  $\sin^2 2_{13}$ – $m_{31}^2$  space, assuming the case of no depletion of flux. The four panels in Fig. 2 correspond to Run I, IIA, IIB, and III. In each panel, the red-solid, the green-dashed, and the blue-dotted lines are for 1 (68.27%), 2 (95.45%), and 3 (99.73%) CL for 1 DOF, respectively. The sensitivities indicated in Fig. 2 is quite impressive, which reach to  $\sin^2 2_{13} \approx 0.006$  at 2 CL even in Run I, and to  $\sin^2 2_{13} \approx 0.004$  at the same CL in Run IIB. As expected the improvement by adding more detector locations is relatively minor.

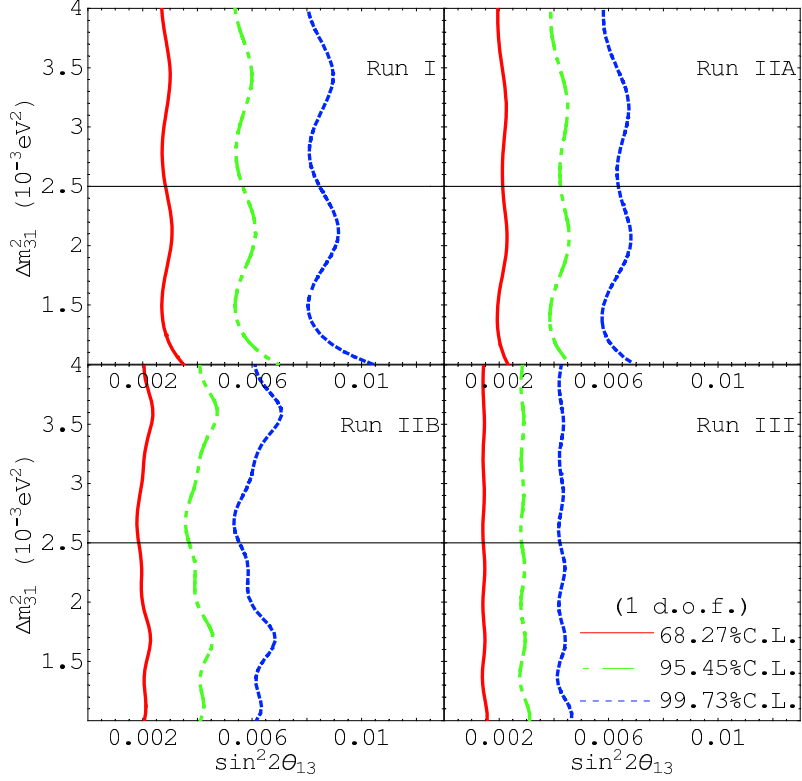


FIG. 2: The sensitivity limit of  $\Delta m_{31}^2$  by Run I, IIA, IIB, and III with number of events  $10^6$  in each location are depicted. The red-solid, the green-dashed, and the blue-dotted lines are for 1 (68.27%), 2 (95.45%), and 3 (99.73%) CL for 1 DOF, respectively.

### B. Case of pessimistic systematic error

Suppose that the direct detection of  ${}^3\text{H}$  in the target is not possible and we take the option of multiple detectors with the same structure. Then, most probably we have to accept a pessimistic value of the uncorrelated systematic error of 1%. Or, it might be possible that we end up with the error of this order anyway even with the direct counting of  ${}^3\text{H}$ . In Fig. 3 we present the similar allowed region in  $\sin^2 2\theta_{13}$  –  $\Delta m_{31}^2$  space obtained by the same Run I, IIA, IIB, and III with the same number of events of  $10^6$  in each location but with a pessimistic systematic error of  $u_{\text{sys}} = 1\%$ . At large  $\theta_{13}$ ,  $\sin^2 2\theta_{13} = 0.1$ , we still have reasonable sensitivities for  $\Delta m_{31}^2$ . For Run IIB and III, for example, the sensitivities are about 1-2% level. At  $\sin^2 2\theta_{13} = 0.01$ , however, the sensitivity to  $\Delta m_{31}^2$  is lost except for the one at 1 CL in Run III. It indicates that the value of  $\theta_{13}$  is close to the sensitivity limit, and hence we do not place the figure for it though we did for the case of optimistic error, Fig. 2.

For more detailed information on sensitivities with the pessimistic systematic error of  $u_{\text{sys}} = 1\%$ , we give in Tables III and IV the sensitivities at 1 and 3 CL (the latter in parentheses) for 1 DOF to  $\Delta m_{31}^2$  and  $\sin^2 2\theta_{13}$ , respectively. The column without number represent that no limit is obtained, in the similar way as seen in the right panels in Fig. 3. At relatively large  $\theta_{13}$ ,  $\sin^2 2\theta_{13} = 0.1$  and 0.05, the sensitivities to  $\Delta m_{31}^2$  remain to be good, 1.2% and 2.4% at 1 CL for Run IIB. But, the sensitivity quickly drops and is about

TABLE III: The expected fractional uncertainty  $(m^2) = m_{31}^2(0)$  in % for the pessimistic systematic error of  $u_{\text{sys}} = 1\%$  reachable by the Run I – III defined in the text. The uncertainties are given at 1 (68.27%) CL for 1 D.O.F., and the numbers in parentheses are the ones at 3 (99.73%) CL for 1 D.O.F. In the left, middle, and right columns, the input value of  $m_{13}$  are taken as  $\sin^2 2_{13} = 0.1$ , 0.05, and 0.01, respectively. The column without number represents that no limit is obtained.

$u_{\text{sys}} = 1\%$	$\sin^2 2_{13} = 0.1$	$\sin^2 2_{13} = 0.05$	$\sin^2 2_{13} = 0.01$	
Run type	$(m^2) = m_{31}^2(0)$ (in %) at 1 (3) CL			
Run I (5 locations)	$+4.0$ $3.6$	$+12$ $10$	$+8.0$ $7.2$	$+27$ $20$
Run IIA (10 locations)	2.4	$+8.0$ $7.2$	5.2	$+16$ $14$
Run IIB (10 locations)	1.2 (3.5)		2.4	$+8.4$ $7.2$
Run III (20 locations)	0.8 (2.4)		1.6 (5.2)	$+9.2$ $8.4$

TABLE IV : The expected sensitivity to the  $\sin^2 2_{13}$  for the pessimistic systematic error of  $u_{\text{sys}} = 1\%$  reachable by the Run I – III defined in the text. The uncertainties ( $\sin^2 2_{13}$ ) are given at 1 (68.27%) CL for 1 D.O.F., and the numbers in parentheses are the ones at 3 (99.73%) CL for 1 D.O.F. In the left, middle, and right columns, the input value of  $m_{13}$  are taken as  $\sin^2 2_{13} = 0.1$ , 0.05, and 0.01, respectively. The column without number represent that no limit is obtained.

$u_{\text{sys}} = 1\%$	$\sin^2 2_{13} = 0.1$	$\sin^2 2_{13} = 0.05$	$\sin^2 2_{13} = 0.01$
Run type	$\sin^2 2_{13}$ at 1 (3) CL		
Run I (5 locations)	0.1 0.011 (0.034)	0.05 0.012 (0.037)	0.01 $+0.013$ $+0.037$
Run IIA (10 locations)	0.1 0.009 (0.026)	0.05 0.009 $+0.027$ $0.022$	0.01 $+0.009$ $+0.028$
Run IIB (10 locations)	0.1 0.007 (0.023)	0.05 0.008 $+0.021$ $0.024$	0.01 0.008 $+0.024$
Run III (20 locations)	0.1 0.006 (0.017)	0.05 0.006 (0.018)	0.01 0.006 $+0.019$

15% in the same Run for  $\sin^2 2_{13} = 0.01$ . The sensitivity to  $\sin^2 2_{13}$  is still reasonable,  $(\sin^2 2_{13})' = 0.008$  at 1 CL for Run IIB even at  $\sin^2 2_{13} = 0.01$ .

For disappearance measurement of  $P(e^+ \rightarrow e^-)$ ,  $\sin^2 2_{13} = 0.01$  is a too small value for a pessimistic systematic error of  $u_{\text{sys}} = 1\%$  to retain the sensitivity to  $m_{31}^2$ . Therefore, reduction of the uncorrelated systematic error is the mandatory requirement in this method for accurate measurement of  $m_{31}^2$  at small  $2_{13}$ .

## V . ANALYTIC ESTIMATION OF THE SENSITIVITIES

We complement our numerical analysis of the sensitivities in the previous section by presenting analytical treatment of the uncertainties in the  $m_{31}^2$  and  $2_{13}$  determination. In particular, we derive analytic formulas for the sensitivities of  $m_{31}^2$  and  $\sin^2 2_{13}$  under the approximation of small uncorrelated systematic error compared to correlated one,  $u^2_u + u^2_c$ . In Sec. III, we have argued, assuming feasible direct counting of  $^3\text{H}$  atoms, that the hierarchy of errors is very likely to hold.

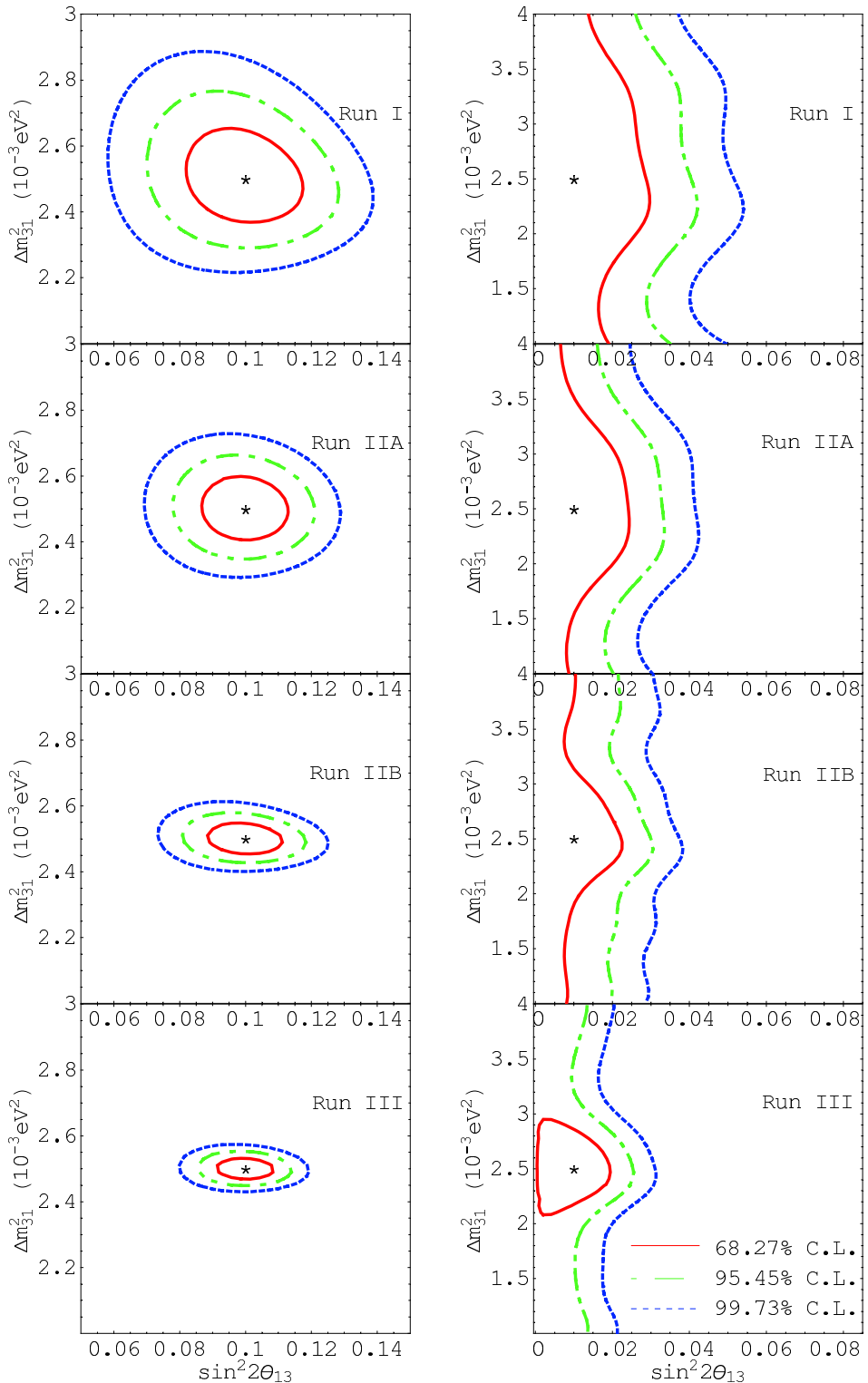


FIG. 3: The same as in Fig. 1 but with the pessimistic systematic error of  $\sigma_{\text{sys}} = 1\%$ . The input values of  $\sin^2 2\theta_{13}$  is taken as 0.1 and 0.01 in the left and the right panels.

We restrict ourselves, in consistent with the numerical analysis done in the previous section, to the case that an equal number of events are taken in each baseline,  $N_i^{\text{obs}} = N^{\text{obs}}$ , which may be translated into  $N_i^{\text{exp}} = N^{\text{exp}}$ . We also assume, for simplicity, the case of equal uncorrelated systematic error in each detector location,  $\frac{2}{u_i} + \frac{2}{u_{\text{sys};i}} + \frac{1}{N_i^{\text{exp}}} = \frac{2}{u}$ . Under these assumptions,  $V^{-1}$  has a simple form

$$V^{-1} = \frac{1}{\frac{2}{u}} I - \frac{1}{n} H_{n,n} = \frac{1}{\frac{2}{u}} \begin{matrix} 0 & 1 & \frac{1}{n} & \frac{1}{n} & \frac{1}{n} & \frac{1}{n} & \frac{1}{n} & 1 \\ B & \frac{1}{n} & 1 & \frac{1}{n} & \frac{1}{n} & \frac{1}{n} & \frac{1}{n} & C \\ \frac{1}{n} & B & \frac{1}{n} & 1 & \frac{1}{n} & \frac{1}{n} & \frac{1}{n} & CC \\ \frac{1}{n} & \frac{1}{n} & B & \frac{1}{n} & 1 & \frac{1}{n} & \frac{1}{n} & CCC \\ \vdots & \vdots A \\ \frac{1}{n} & 1 \end{matrix}; \quad (12)$$

where  $H_{n,n}$  is an  $n \times n$  matrix whose elements are all unity,  $H_{i,j} = 1$  for any  $i$  and  $j$ . It indicates again the independence of the  $\frac{2}{c}$  on the correlated error  $\frac{2}{c}$  and the 'scaling behavior' with respect to the uncorrelated systematic error. Then, the  $\frac{2}{c}$  simplifies:

$$\frac{2}{c} = \frac{1}{\frac{n}{u}} \frac{X^n}{\prod_{i,j=1}^n} \frac{N_i^{\text{obs}}}{N_i^{\text{exp}}} \frac{N_j^{\text{obs}}}{N_j^{\text{exp}}} \dots \frac{!_2}{!}; \quad (13)$$

#### A. Optimal baselines and sensitivities for two detector locations

Let us start by examining sensitivities for the case of two detector locations. Because of a simple setting with monochromatic  $e$  beam we can give explicit expression of  $\frac{2}{c}$  in terms of small deviation of the parameters from the true (nature's) values. For this purpose, we note that the number of events is given by

$$N^{\text{exp}}(N^{\text{obs}}) = f_e \text{res} N_T T P_{ee}(\theta_{13}; m_{31}^2; L); \quad (14)$$

where  $f_e$  denotes the neutrino flux,  $\text{res}$  the absorption cross section,  $N_T$  the number of target nuclei,  $T$  the running time, and  $P_{ee}$  is a short-hand notation for  $P(e \rightarrow e)$ . In the setting in this section,  $T$  is adjusted such that an equal number of events is collected at each location of the detector. We recall that  $N^{\text{obs}}$  denotes the event number computed with the true value of the parameters,  $m_{31}^2 = m^2(0)$  and  $\sin^2 \theta_{13} = \sin^2 \theta_{13}(0)$ , whereas  $N^{\text{exp}}$  denotes the event number computed with possible small deviations ( $m^2$ ) and ( $\sin^2 \theta_{13}$ ) from the true values of the parameter. Then,  $i$ -th component of  $\mathbf{x}$  vector in (9) is given to first order in the deviation as

$$\frac{N_i^{\text{obs}}}{N_i^{\text{exp}}} - 1 = \frac{1}{P_{ee}^{(0)}(L_i)} \sin^2 \frac{m_{31}^2(0)L_i}{4E} (\sin^2 \theta_{13}) + \frac{1}{2} \sin^2 \theta_{13}(0) \sin \frac{m_{31}^2(0)L_i}{2E} \frac{(m^2)L_i}{2E}; \quad (15)$$

where  $P_{ee}^{(0)}(L_i) = P_{ee}[\theta_{13}(0); m_{31}^2(0); L_i]$  for which we have used the two-avor expression (2).

For simplicity we restrict our discussion in this section to the analysis with single degree of freedom. It is a natural setting for estimating ultimate sensitivities; when we discuss

sensitivity of  $m_{31}^2$  we optimize  $\sin^2 2_{13}$  in terms of  $\sin^2 2_{13}$ , and vice versa. Or, one can think of the situation in which  $\sin^2 2_{13}$  is accurately determined by other ways, e.g., long-baseline accelerator experiments in the determination of  $m_{31}^2$ .

Under the approximation  $\sin^2 2_{13} \approx \sin^2 2_{31}$  and using  $V^{-1}$  in (12),  $\sin^2 2_{13}$  is given for small deviations of  $\sin^2 2_{13}$  and  $m_{31}^2$  as follows:

$$\sin^2 2_{13} = \frac{2}{2 \sin^2 \theta_u} \frac{[\sin^2 2_{13}(0)]^2}{4 \frac{\sin^2 \frac{m_{31}^2(0)L_1}{4E}}{P_{ee}^{(0)}(L_1)}} \frac{\sin^2 \frac{m_{31}^2(0)L_2}{4E}}{P_{ee}^{(0)}(L_2)} \frac{3_2}{5}; \quad (16)$$

$$\frac{m_{31}^2}{2} = \frac{\frac{[\sin^2 2_{13}(0)]^2}{8 \sin^2 \theta_u} \frac{(m_{31}^2)^2}{m_{31}^2(0)}}{4 \frac{\frac{m_{31}^2(0)L_1}{2E} \sin \frac{m_{31}^2(0)L_1}{2E}}{P_{ee}^{(0)}(L_1)}} \frac{\frac{m_{31}^2(0)L_2}{2E} \sin \frac{m_{31}^2(0)L_2}{2E}}{P_{ee}^{(0)}(L_2)} \frac{3_2}{5}; \quad (17)$$

Now, we can address the problem of optimal baseline and estimate the sensitivities of  $\sin^2 2_{13}$  and  $m_{31}^2$  under the approximations stated above. Since  $\sin^2 2_{13} < 0.1$  [29] it may a reasonable approximation to set  $P_{ee}^{(0)}(L_i) = 1$  in the denominator, as we do in the rest of the section.

### 1. Optimal setting and sensitivity for $\sin^2 2_{13}$

To maximize (16) one should take  $L_1$  as short as possible, and  $L_2$  at the oscillation maximum, the well known feature in the reactor  $\sin^2 2_{13}$  experiments. Thus, we take  $L_1 = 0$  and  $L_2 = L_{OM}$  which makes the square parenthesis in (16) unity. Then, one can obtain the sensitivity at  $N_{CL}$  CL for 2 detector locations as

$$(\sin^2 2_{13}) = \frac{2N_{CL} \frac{\theta_u}{2}}{2} = \frac{2N_{CL}}{2} \frac{\frac{\theta_{sys}^2 + \frac{1}{N}}{2}}{2}; \quad (18)$$

For  $\theta_u = 0.2\%$ ,  $(\sin^2 2_{13}) = 2.8 \times 10^3$  ( $8.5 \times 10^3$ ) at 1 (3) CL. For  $\theta_u = 1\%$ ,  $(\sin^2 2_{13}) = 0.014$  (0.043) at 1 (3) CL, which is not so far from the sensitivities quoted in the literatures of the reactor  $\sin^2 2_{13}$  experiments.

### 2. Optimal setting and sensitivity for $m_{31}^2$

The optimal baseline setting is quite different for  $m_{31}^2$ . We first recall a property of the function  $x \sin x$ ; It has the first maximum  $x \sin x = 1.82$  at  $x = 2.02$  ( $L = 0.64L_{OM}$ ), has the first minimum  $x \sin x = -4.81$  at  $x = 4.91$  ( $L = 1.56L_{OM}$ ), and then, the second maximum  $x \sin x = 7.92$  at  $x = 7.98$  ( $L = 2.54L_{OM}$ ). Notice that we restrict ourselves to  $x < 3$ , which means  $L < 3L_{OM}$  so that the running time does not blow up. Then, the optimal setting is  $L_1 = 0.64L_{OM}$  and  $L_2 = 1.56L_{OM}$  if we restrict to  $L < 2L_{OM}$ , and  $L_1 = 1.56L_{OM}$  and  $L_2 = 2.54L_{OM}$  if we allow baseline until  $L = 3L_{OM}$ . Despite the factor of

4 different baseline lengths, we still assume the equal numbers of events at  $L = 0.64L_{OM}$  and  $L = 2.54L_{OM}$ , which implies 16 times longer exposure time at the latter distance.

The  $\chi^2$  is given approximately by

$$\chi^2_{m^2} = \frac{C}{u} \sin^4 2_{13}(0) \frac{(m^2_{31})^2}{m^2_{31}(0)} : \quad (19)$$

The coefficient  $C$  is 5.5 for  $L = 2L_{OM}$  and 20.3 for  $L = 3L_{OM}$ . Then, we obtain the sensitivity at  $N_{CL}$  CL for 2 detector locations as

$$\frac{(m^2_{31})}{m^2_{31}(0)} = \frac{1}{\sin^2 2_{13}(0)} N_{CL} p_{\frac{u}{C}}; \quad (20)$$

Hence, the sensitivity to  $m^2_{31}$  depends very sensitively on  $\sin^2 2_{13}$ .

With  $u = 0.2\%$ ,  $\frac{(m^2_{31})}{m^2_{31}(0)} = 8.5 \cdot 10^3$  at 1 CL for  $\sin^2 2_{13} = 0.1$  if we restrict to  $L = 2L_{OM}$ . If we allow  $L = 3L_{OM}$ , the sensitivity becomes better,  $\frac{(m^2_{31})}{m^2_{31}(0)} = 4.4 \cdot 10^3$  at the same CL. If the systematic error is worse,  $u = 1\%$ , the sensitivity at  $\sin^2 2_{13} = 0.1$  becomes to  $\frac{(m^2_{31})}{m^2_{31}(0)} = 4.3 \cdot 10^2$  and  $\frac{(m^2_{31})}{m^2_{31}(0)} = 2.2 \cdot 10^2$  for  $L = 2L_{OM}$  and  $L = 3L_{OM}$  cases, respectively, at 1 CL.

## B. The problem of $n$ detector locations reduces to 2 location case

We first show that the problem of optimal setting of  $n$  detector locations reduces to the case of 2 locations under the assumption of equal number of events in each location. To indicate the essential point let us first consider a simplified  $\chi^2$  of the form  $\chi^2 = \sum_{i,j=1}^n (x_i - x_j)^2$  and  $0 \leq x_i \leq 1$ , which is the essential part of  $\chi^2$  for  $\sin^2 2_{13}$ , (16). In the case of 2 locations the configuration which maximizes the  $\chi^2$  ( $n = 2$ ) is  $x_1 = 0$  and  $x_2 = 1$  and  $\chi^2_{max}(n=2) = 1$ . It is not difficult to observe that in the case of  $n$ -locations the configuration which maximizes  $\chi^2$  ( $n$ ) is

Even  $n: n=2M$ ;  $x=0$  appears  $M$  times, and  $x=1$  appears  $M$  times,  $\chi^2(n)_{max} = M^2$ .

Odd  $n: n=2M+1$ ;  $x=0$  appears  $M+1$  times, and  $x=1$  appears  $M$  times, or vice versa,  $\chi^2(n)_{max} = M(M+1)$ .

Thus, the problem of optimal setting with equal number of events at each detector location is reduced to the 2 location case.

For  $\chi^2$  for  $m^2_{31}$  in (17) the situation is slightly different because the function  $\chi \sin x_j$  increases without limit as  $x$  becomes large. Therefore, mathematically speaking, one can obtain better and better accuracies as one goes to longer and longer distances in our setting of equal number of events at any detector location.<sup>2</sup> But, since we want to remain to a reasonable running time, we have restricted our discussions to baselines limited by  $L = 2L_{OM}$  or  $L = 3L_{OM}$  in the 2 location case, the restriction which is kept throughout this section.

<sup>2</sup> This explains at least partly the reason why the sensitivities to  $m^2_{31}$  and  $\sin^2 2_{13}$  differ in dependence on distance from the source to a detector, as indicated in Fig. 3 in [30].

Then, one can show that the same result follows for  $m_{31}^2$  for  $m_{31}^2$ , (17). Namely, in the case of  $n$  locations, the highest sensitivity is achieved at the same baselines  $L_1$  and  $L_2$  of the 2 location case;  $L_1$  in  $\frac{n}{2}$  ( $\frac{n}{2} + 1$  for odd  $n$ ) times, and  $L_2$  in  $\frac{n}{2}$  times, where  $[ ]$  implies Gauss' symbol.

The maximal value of  $m_{31}^2$  is, therefore, given by

$$\begin{aligned} {}^2(n)_{\max} &= \frac{n}{2} {}^2(n=2)_{\max}; \text{(even } n\text{)}; \\ {}^2(n)_{\max} &= \frac{n^2 - 1}{2n} {}^2(n=2)_{\max}; \text{(odd } n\text{)}; \end{aligned} \quad (21)$$

It can be translated into the uncertainties at  $N_{CL}$  CL as

$$\begin{aligned} (\sin^2 2_{13})(n) &= \frac{r}{2} (\sin^2 2_{13})(n=2); \\ \frac{(\sin^2 2_{13})(n)}{m_{31}^2(0)} &= \frac{r}{n} \frac{(\sin^2 2_{13})(n=2)}{m_{31}^2(0)}; \end{aligned} \quad (22)$$

for even  $n$ . For odd  $n$ ,  $n$  in (22) must be replaced by  $\frac{n^2 - 1}{n}$ .  $(\sin^2 2_{13})(n=2)$  and  $\frac{(\sin^2 2_{13})(n)}{m_{31}^2(0)}$  ( $n=2$ ) are given respectively by (18) and (20). Therefore, the sensitivity gradually improves as number of runs becomes larger.<sup>3</sup>

At the end of this subsection, we want to note the following: The reason why we did not take these sets of the optimal distances for  $2_{13}$  and  $m_{31}^2$  obtained in this subsection in the numerical analyses in Sec. IV is that the sensitivity to  $m_{31}^2$  is lost if we tune the setting optimal for  $\sin^2 2_{13}$ , and vice versa. Nonetheless, we will see, in the following subsections, that the sensitivities analytically estimated with optimal baseline distances and the numerically calculated ones with baselines taken by "common sense" agree reasonably well with each other.

### C. Analytic estimation of the sensitivities; $\sin^2 2_{13}$

Let us examine the case of  $u_{\text{sys}} = 0.2\%$  and the number of events  $N = 10^6$  which was considered in our numerical analysis in Sec. IV. Then,  $u = 0.22\%$ . In the case of 5 locations,  $n = 5$ ,  $(\sin^2 2_{13}) = 2.0 \cdot 10^3$  ( $6.1 \cdot 10^3$ ) at 1 (3) CL. Similarly for 10 and 20 locations  $(\sin^2 2_{13}) = 1.4 \cdot 10^3$  ( $4.2 \cdot 10^3$ ) and  $0.99 \cdot 10^3$  ( $3.0 \cdot 10^3$ ), respectively, at 1 (3) CL. They compare well with the numbers in Table II though the latter are obtained with not-so-tuned baseline settings. Notice that  $(\sin^2 2_{13})$  is independent of  $2_{13}$  under the present approximation of small deviation from the best  $t$ .

With  $u_{\text{sys}} = 1\%$  the corresponding sensitivities are  $(\sin^2 2_{13}) = 9.2 \cdot 10^3$  ( $2.8 \cdot 10^2$ ),  $6.4 \cdot 10^3$  ( $1.9 \cdot 10^2$ ), and  $4.5 \cdot 10^3$  ( $1.3 \cdot 10^2$ ) for 5, 10, and 20 locations, respectively, at 1 (3) CL. They are again roughly consistent with the ones in Table IV.

<sup>3</sup> It is the well known feature in the multiple detector setting in the reactor  $2_{13}$  experiments in which one obtains better sensitivity as in (18) if the two identical detectors, the near and the far, are each divided into small detectors in the same way, if the uncorrelated systematic error  $u_{\text{sys}}$  is made to be equal with that of the original large detector and if the statistical errors are negligible even for divided detectors. This point was emphasized by Yasuda [31].

TABLE V : The analytically estimated fractional uncertainties of  $m_{31}^2$ ,  $(m^2) = m_{31}^2(0)$  in % are given for the optimistic systematic error of  $u_{sys} = 0.2\%$  and for the pessimistic one (in parentheses) of  $u_{sys} = 1\%$ . The uncertainties are given at 1 (68.27%) CL for 1 DOF for the cases of 5, 10, and 20 detector locations. The upper three rows are for the case of restricted baselines,  $L = 2L_{OM}$ , whereas the lower three rows are for the cases of somewhat relaxed baseline setting,  $L = 3L_{OM}$ . In the left, middle, and right columns, the input value of  $\sin^2 2_{13}$  are taken as  $\sin^2 2_{13} = 0.1$ , 0.05, and 0.01, respectively.

$L = 2L_{OM}$	$u_{sys} = 0.2\% \quad (u_{sys} = 1\%)$		
number of locations	$(m^2) = m_{31}^2(0)$ (in %) at 1 CL		
	$\sin^2 2_{13} = 0.1$	$\sin^2 2_{13} = 0.05$	$\sin^2 2_{13} = 0.01$
5 locations	0.61 (2.8)	1.2 (5.5)	6.1 (28)
10 locations	0.42 (1.9)	0.85 (3.8)	4.2 (19)
20 locations	0.30 (1.3)	0.6 (2.7)	3.0 (13)
$L = 3L_{OM}$	$(m^2) = m_{31}^2(0)$ (in %) at 1 CL		
5 locations	0.32 (1.5)	0.62 (2.9)	3.2 (15)
10 locations	0.22 (0.99)	0.44 (2.0)	2.2 (9.9)
20 locations	0.15 (0.68)	0.31 (1.4)	1.5 (6.8)

#### D . Analytic estimation of the sensitivities; $m_{31}^2$

We examine the case of severer restriction  $L = 2L_{OM}$  and the milder one  $L = 3L_{OM}$ . In the first case, the maximum of the function  $x \sin x$  is at  $x = 2.02$  ( $L = 0.64L_{OM}$ ) where  $x \sin x = 1.82$ , and the minimum at  $x = 4.91$  ( $L = 1.56L_{OM}$ ) where  $x \sin x = -4.81$ . In the case of milder restriction  $L = 3L_{OM}$ , the maximum of the function  $x \sin x$  is at  $x = 7.98$  ( $L = 2.54L_{OM}$ ) where  $x \sin x = 7.92$ , and the minimum at  $x = 4.91$  ( $L = 1.56L_{OM}$ ) as above.

In Table V, we give the fractional uncertainties of  $m_{31}^2$ ,  $(m^2) = m_{31}^2(0)$  in % at 1 CL for the optimistic and the pessimistic systematic error of  $u_{sys} = 0.2\%$  and  $1\%$ , respectively, obtained by using the equations (20) and (22). (We do not show errors at 3 CL because it is obtained by multiplying 3.) Overall, the analytically estimated uncertainties are in reasonable agreement with those obtained by the numerical analysis in Sec. IV. Notice that one has to compare the sensitivities of Run I and IIA with the case of severer restriction  $L = 2L_{OM}$ , and the ones of Run IIB and III with the case of milder restriction  $L = 3L_{OM}$ , because distances beyond  $2L_{OM}$  are involved in the latter runs. The fact that our analytical estimates of the errors are smaller than the numerical ones by 30% or so, apart from approximations involved, is consistent with that the latter are based on non-optimal baseline distances. It also implies that the baseline setting chosen by the 'common sense' used in the numerical analysis in Sec. IV is not so far from the optimal one, indicating that the sensitivities are rather stable against changes of baseline setting.

Based on the numerical and the analytical estimate of the uncertainties of  $m_{31}^2$  determination, we can conclude that 1% -level sensitivity at 90% CL required for resolution of mass hierarchy proposed in [10, 11] is in reach if  $\sin^2 2_{13}$  is relatively large,  $\sin^2 2_{13} > 0.05$  in Run IIB and if the uncorrelated systematic error of  $u_{sys} = 0.2\%$  is realized.

We have confined ourselves to the problem of optimal setting of distances under the constraint of equal number of events at each location. To minimize running time for a given sensitivity, we have to address the problem of optimal detector locations for a given running time. It is left for a future study.

## V I. CONCLUDING REMARKS

In this paper, we have explored the potential of high sensitivity measurement of  $m_{31}^2$  and  $m_{13}$  which is enabled by using the resonant absorption of monochromatic  $e$  beam enhanced by the Mössbauer effect. With baseline distances of 10 m, the movable detector setting is certainly possible. Assuming that the direct detection of produced  ${}^3H$  atom either by real time counting or extraction of  ${}^3H$  atoms works, we have argued that the uncorrelated systematic error can be as small as 0.1% - 0.3%, if there equipped a near detector with the same structure with the far one. It will allow us to determine  $m_{31}^2$  to less than 1% level at 1 CL for  $\sin^2 2_{13} = 0.03$  (Run IIB,  $u_{\text{sys}} = 0.2\%$ ). The error of  $\sin^2 2_{13}$  is also small,  $\sin^2 2_{13} = 1.8 \cdot 10^3$  almost independently of  ${}_{13}$  with the same setting.

What is the scientific merit of the precision measurement of  $m_{31}^2$  and  ${}_{13}$ ? As we have already mentioned in Sec. I the precision measurement of  $m_{31}^2$  and  ${}_{13}$  will have a great impact to, at least, the two of the unknowns in the lepton flavor mixing, the neutrino mass hierarchy and resolving the  ${}_{23}$  octant degeneracy. It would be very interesting to carry out quantitative analyses of such possibilities. It should also be stressed that such physics capabilities can only be made possible by the direct counting of the produced  ${}^3H$  atoms. We hope that these exciting possibilities stimulate further development of the experimental technology toward the goal.

The accuracy of the  ${}_{13}$  measurement with resonant  $e$  absorption, even in Run I, is comparable with that of the accelerator  $e$  appearance experiments [19, 32], if the systematic error of 0.2% is reached. It may exceed the accelerator sensitivity if Run IIB is performed. If the systematic error is of 1% level, the sensitivity to  ${}_{13}$  is similar to the first-stage reactor  ${}_{13}$  experiments even in Run IIB.

What are the additional capabilities of the resonant absorption of monochromatic  $e$  beam? With 18.6 keV of neutrino energy the solar oscillation maximum would be reached at  $L_{\text{solarOM}} = 290 \cdot \frac{m_{21}^2}{8 \cdot 10^{-5} \text{ eV}^2} \text{ m}^1$ . Then, it would be worthwhile to explore the possibility of precision measurement of  ${}_{12}$  and  $m_{21}^2$ , as was done for the reactor experiments [30]. But, in the present case, neither geo-neutrinos nor  $e$  flux from nearby reactors (if any) contaminate the measurement. In particular, possible movable or multiple baseline set up should allow improvement of accuracy of  $m_{21}^2$  determination.

Despite great sensitivities achievable by the resonant absorption reaction, detection of CP violating effect due to  $e$  disappearance measurement requires to go down by a factor of  $0.1 (10^{-6})$  compared to CP conserving terms, unfortunately [33].

Finally, the setup of multiple baseline lengths of 10 m allows a precision test of the pure vacuum oscillation hypothesis by observing a sine curve slightly modified by the solar  $m_{21}^2$  oscillation. It will constrain various possible sub-leading effects such as de-coherence or new neutrino interactions to a great precision.

## APPENDIX A: GENERAL FORMULA FOR $\chi^2$ FOR n-UNCORRELATED AND -CORRELATED ERRORS

We consider a general setting with  $n$ -uncorrelated and  $\gamma$ -correlated errors.  $\hat{\beta}$  is given in a form as

$$^2 = \mathbf{x}^T V^{-1} \mathbf{x} \quad (\text{A } 1)$$

where  $\mathbf{x}^T = (x_1; x_2; \dots; x_n)$  and  $x_i = \frac{\sum_{j=1}^{N_i} \text{obs}_j}{N_i \text{exp}}$ . We also introduce a vector notation for parameters  $\mathbf{p} = (p_1; p_2; \dots)$  for correlated error as  $\mathbf{v}^T = (v_1; v_2; \dots)$  for so called the 'pull type' [34, 35]. Then,  $\mathbf{v}^2$  can be written [22]

After minimization by  $j, V^1$  can be written as

$$V^{-1} = D_u^{-1} D_u^{-1} H A^{-1} H^T D_u^{-1} : \quad (A3)$$

In the above equations,  $D_u$  is an  $n \times n$  matrix  $D_u = \text{diag}(\frac{2}{u_1}, \dots, \frac{2}{u_n})$ ;  $D_c$  is an  $n \times m$  matrix  $D_c = \text{diag}(\frac{2}{c_1}, \dots, \frac{2}{c_n})$ ; and  $H$  is an  $n \times m$  matrix whose elements are all unity,  $H_{p,i} = 1$  for any  $p = 1, \dots, n$  and  $i = 1, \dots, m$ . Finally, the  $n \times m$  matrix  $A$  is defined by

$$A = D_c^{-1} + H^T D_u^{-1} H \quad (A 4)$$

Note that the statistical errors are incorporated in the uncorrelated errors as  $\frac{1}{N_i \exp}$ . A simple "path-integral" proof is given by [22] that  $V = D_u + H D_c H^T$ .

Here, we are interested in obtaining the explicit form of  $V^{-1}$  in (A3). We first compute  $A^{-1}$ . We note that the matrix  $A$  given in (A4) can be written explicitly as

$$A = \frac{X^n - \frac{1}{2}}{u_i} T; \quad (A 5)$$

$$T = \begin{matrix} 0 & & & & & 1 \\ & 1 + & 1 & 1 & & 1 \\ & & 1 & 1 + & 2 & 1 \\ & & & 1 & & 1 \\ & & & & 1 + & 3 \\ & & & & & 1 \\ \vdots & \vdots & \vdots & \vdots & \vdots & \vdots \\ & 1 & 1 & 1 & & 1 + \end{matrix}; \quad (A.6)$$

where  $i$  in (A 6) is given by

$$p = \frac{1}{\sum_{i=1}^n u_i} \frac{x^n}{\prod_{i=1}^n u_i} \quad (p = 1; \dots) \quad (A.7)$$

It is easy to show that  $T^{-1}$  is given as

$$(T^{-1})_{pp} = \frac{1}{p} \frac{h}{1 + \sum_{r=1}^{\infty} \frac{1}{r}} = \frac{1}{p} \frac{h}{1 + \frac{2}{p}}; \quad (A8)$$

$$(T^{-1})_{pq} = \frac{1}{p} \frac{h}{1 + \sum_{r=1}^{\infty} \frac{1}{r}} \quad (p \neq q); \quad (A9)$$

Then, the second term of  $V^{-1}$  in (A3) is given by

$$\begin{aligned} (V_{\text{2nd term}}^{-1})_{ij} &= \frac{1}{\frac{2}{2} \frac{u_i u_j}{u_i u_j}} \sum_p X^p H_{ip} (A^{-1})_{pp} H_{pj} + \sum_{p \neq q} X^p H_{ip} (A^{-1})_{pq} H_{qj}; \\ &= \frac{1}{\frac{2}{2} \frac{u_i u_j}{u_i u_j}} \sum_p X^p (A^{-1})_{pp} + \sum_{p \neq q} X^p (A^{-1})_{pq}; \end{aligned} \quad (A10)$$

We thus obtain  $V^{-1}$  as

$$(V^{-1})_{ij} = \frac{1}{\frac{2}{2} \frac{u_i u_j}{u_i u_j}} \frac{h}{1 + \sum_{k=1}^n \frac{1}{\frac{2}{2} u_k}} \sum_{p=1}^{\frac{2}{2} \frac{u_i u_j}{u_i u_j}} X^p (A^{-1})_{pp} + \sum_{p=1}^{\frac{2}{2} \frac{u_i u_j}{u_i u_j}} X^p (A^{-1})_{pq}; \quad (A11)$$

#### ACKNOWLEDGMENTS

We thank Hiro Sugiyama and O사무 Yasuda for informative correspondences and helpful discussions on statistical procedure for our analysis. One of the authors (H.M.) thanks Abdus Salam International Center for Theoretical Physics for hospitality where this work is completed. This work was supported in part by the Grant-in-Aid for Scientific Research, No. 16340078, Japan Society for the Promotion of Science.

---

[1] R.S. Raghavan, arXiv:hep-ph/0511191.  
 [2] R.S. Raghavan, arXiv:hep-ph/0601079.  
 [3] L.A. Mikaelyan, B.G. Tsinov, and A.A. Borovoi, Sov. J. Nucl. Phys. 6, 254 (1968) [Yad. Fiz. 6, 349 (1967)].  
 [4] Y.K. Ozlov, L.M. Mikaelyan and V.S. Sinev, Phys. Atom. Nucl. 66, 469 (2003) [Yad. Fiz. 66, 497 (2003)] [arXiv:hep-ph/0109277].  
 [5] H.M. Inakata, H. Sugiyama, O. Yasuda, K. Inoue and F. Suekane, Phys. Rev. D 68, 033017 (2003) [Erratum -ibid. D 70, 059901 (2004)] [arXiv:hep-ph/0211111].  
 [6] K. Anderson et al., White Paper Report on Using Nuclear Reactors to Search for a Value of  $13$ , arXiv:hep-ex/0402041.  
 [7] R.L. Mössbauer, Z. Physik 151, 124 (1958).  
 H. Frauenfelder, The Mössbauer Effect (Benjamin, 1962).  
 [8] R.V. Pound and G.A. Rebka, Phys. Rev. Lett. 4, 337 (1960); R.V. Pound and J.L. Snider, Phys. Rev. Lett. 13, 539 (1964).

[9] M . H . Shaevitz and J. M . Link, arX iv:hep-ex/0306031, in Proceedings of 4th Workshop on Neutrino Oscillations and Their Origin (NOON 2003), edited by Y . Suzuki, M . Nakahata, Y . Itow, M . Shiozawa, and Y . Obayashi (World Scientific, Singapore, 2004) pp.171

[10] H . Nunokawa, S . Parke and R . Zukanovich Funchal, Phys. Rev. D 72, 013009 (2005) [arX iv:hep-ph/0503283].

[11] A . de Gouvea, J . Jenkins and B . Kayser, arX iv:hep-ph/0503079.

[12] G . Fogli and E . Lisi, Phys. Rev. D 54, 3667 (1996); [arX iv:hep-ph/9604415].

[13] G . Barenboim and A . de Gouvea, arX iv:hep-ph/0209117.

[14] K . H iraide, H . M inakata, T . Nakaya, H . Nunokawa, H . Sugiyama, W . J. C . Teves and R . Z . Funchal, arX iv:hep-ph/0601258.

[15] H . M inakata, Phys. Rev. D 52, 6630 (1995) [arX iv:hep-ph/9503417]; Phys. Lett. B 356, 61 (1995) [arX iv:hep-ph/9504222]; S. M . Bilenky, A . Bottino, C . Giunti, and C . W . Kim, Phys. Lett. B 356, 273 (1995) [arX iv:hep-ph/9504405]; K . S . Babu, J. C . Pati, and F . W . Wilczek, Phys. Lett. B 359, 351 (1995) [arX iv:hep-ph/9505334]; G . L . Fogli, E . Lisi, and G . Scioscia, Phys. Rev. D 52, 5334 (1995) [arX iv:hep-ph/9506350].

[16] Y . Fukuda et al. [Super-Kamiokande Collaboration], Phys. Rev. Lett. 81, 1562 (1998) [arX iv:hep-ex/9807003]; Y . Ashie et al. [Super-Kamiokande Collaboration], Phys. Rev. Lett. 93 (2004) 101801 [arX iv:hep-ex/0404034]; Y . Ashie et al. [Super-Kamiokande Collaboration], Phys. Rev. D 71, 112005 (2005) [arX iv:hep-ex/0501064].

[17] M . H . Ahn et al. [K2K Collaboration], Phys. Rev. Lett. 90, 041801 (2003) [arX iv:hep-ex/0212007]; E . Liu et al. [K2K Collaboration], Phys. Rev. Lett. 94, 081802 (2005) [arX iv:hep-ex/0411038].

[18] The MINOS Collaboration, P . Adamson et al., MINOS Detectors Technical Design Report, Version 1.0, NuMIL-337, October 1998.

[19] Y . Itow et al., arX iv:hep-ex/0106019. For an updated version, see:  
<http://neutrino.kek.jp/jfnu/loi/lbiv2.030528.pdf>

[20] J. N . Bahcall, Phys. Rev. 124, 495 (1961)

[21] LBNL Isotopes Project – LUND University Nuclear Data Dissemination Home Page;  
<http://ie.lbl.gov/toi.htm>

[22] H . Sugiyama, O . Yasuda, F . Suekane and G . A . Horton-Smith, arX iv:hep-ph/0409109.

[23] T . Bolton [Braidwood Collaboration], Nucl. Phys. Proc. Suppl. 149, 166 (2005); Braidwood Project Description, available in:  
<http://braidwood.uchicago.edu/>

[24] J . Cao [Daya Bay Collaboration], arX iv:hep-ex/0509041.

[25] J . C . Anjos et al., [Angera Collaboration], arX iv:hep-ex/0511059.

[26] F . Ardellier et al. [Double-Chooz Collaboration], arX iv:hep-ex/0405032.

[27] F . Suekane [KASKA Collaboration], arX iv:hep-ex/0407016.

[28] H . M inakata and H . Sugiyama, Phys. Lett. B 580, 216 (2004) [arX iv:hep-ph/0309323].

[29] M . Apollonio et al. [CHOOZ Collaboration], Phys. Lett. B 420, 397 (1998) [arX iv:hep-ex/9711002]; ibid. B 466, 415 (1999) [arX iv:hep-ex/9907037]. See also, The Palo Verde Collaboration, F . Boehm et al., Phys. Rev. D 64 (2001) 112001 [arX iv:hep-ex/0107009].

[30] H . M inakata, H . Nunokawa, W . J. C . Teves and R . Zukanovich Funchal, Phys. Rev. D 71, 013005 (2005) [arX iv:hep-ph/0407326]; Nucl. Phys. Proc. Suppl. 145, 45 (2005) [arX iv:hep-ph/0501250].

[31] O . Yasuda, arX iv:hep-ph/0403162; private communications.

[32] D . S . Ayres et al. [NOvA Collaboration], arX iv:hep-ex/0503053.

- [33] H. M. Inakata and S. Watanabe, *Phys. Lett. B* **468**, 256 (1999) [[arXiv:hep-ph/9906530](https://arxiv.org/abs/hep-ph/9906530)].
- [34] G. L. Fogli, E. Lisi, A. M. Marrone, D. M. Montanino and A. Palazzo, *Phys. Rev. D* **66**, 053010 (2002) [[arXiv:hep-ph/0206162](https://arxiv.org/abs/hep-ph/0206162)];
- [35] D. Stump et al., *Phys. Rev. D* **65**, 014012 (2002) [[arXiv:hep-ph/0101051](https://arxiv.org/abs/hep-ph/0101051)]; M. Botje, *J. Phys. G* **28**, 779 (2002) [[arXiv:hep-ph/0110123](https://arxiv.org/abs/hep-ph/0110123)]; J. Pumplin, D. R. Stump, J. Huston, H. L. Lai, P. N. Adolsky and W. K. Tung, *JHEP* **0207**, 012 (2002) [[arXiv:hep-ph/0201195](https://arxiv.org/abs/hep-ph/0201195)].